U.S. National Library of Medicine
National Center for Biotechnology Information

NLM Citation: Leung K. ^{99m}Tc-Hydrazinonicotinic acid-bitistatin. 2007 Jul 7 [Updated 2012 Apr 25]. In: Molecular Imaging and Contrast Agent Database (MICAD) [Internet]. Bethesda (MD): National Center for Biotechnology Information (US); 2004-2013.
Bookshelf URL: https://www.ncbi.nlm.nih.gov/books/

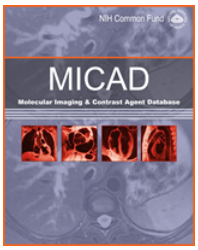

^{99m}Tc-Hydrazinonicotinic acid-bitistatin

^{99m}Tc-HYNIC-bitistatin

Kam Leung, PhD[1]

Created: July 7, 2007; Updated: April 25, 2012.

Chemical name:	^{99m}Tc-Hydrazinonicotinic acid-bitistatin	
Abbreviated name:	^{99m}Tc-HYNIC-bitistatin	
Synonym:		
Agent category:	Polypeptide	
Target:	Platelet glycoprotein GPIIb/IIIa receptor (CD61/CD41)	
Target category:	Receptor	
Method of detection:	Single-photon emission computed tomography (SPECT), gamma planar imaging	
Source of signal:	^{99m}Tc	
Activation:	No	
Studies:	• *In vitro* • Rodents • Humans	Structure is not available in PubChem.

Background

[PubMed]

Thrombosis plays a major role in many cardiovascular diseases such as myocardial infarction, pulmonary embolism (PE), deep venous thrombosis (DVT), or cerebral venous thrombosis (1, 2). DVT is a significant source of PE, which is a potentially life-threatening clinical problem. Thrombosis occurs when platelets deposit in regions of low flow in the deep venous system, followed by an activation process of thrombin, which then converts fibrinogen into fibrin. Platelets become activated and bind to fibrinogen, resulting in platelet aggregation. The thrombus may become organized or detached from the vessel wall. Bitistatin (83 amino acids) belongs to a family of platelet glycoprotein GPIIb/IIIa ligands called disintegrins, which contain an Arg-Gly-Asp (RGD) tripeptide sequence (3). Bitistatin has been shown to inhibit platelet deposition in coronary arteries in a canine model of repetitive thrombus formation (4). ^{99m}Tc-Hydrazinonicotinic acid-bitistatin (^{99m}Tc-HYNIC-bitistatin) is being developed as a single-photon emission computed tomography (SPECT) imaging probe for imaging of acute thrombi and emboli in humans.

Author Affiliation: 1 National for Biotechnology Information, NLM, NIH, Bethesda, MD; Email: micad@ncbi.nlm.nih.gov.

Corresponding author.

Related Resource Links:

- Chapters in MICAD (GPIIb)
- Gene information in NCBI (GPIIIa/CD61, GPIIb/CD41)
- Articles in Online Mendelian Inheritance in Man (OMIM) (GPIIIa/CD61, GPIIb/CD41)
- Clinical trials (Integrin)
- Drug information in FDA (Integrin)

Synthesis

[PubMed]

Knight et al. (5) reported a two-step synthesis of ^{99m}Tc-HYNIC-bitistatin using the bifunctional chelating agent *N*-succinimidyl-HYNIC, a ligand with two active sites: one for protein conjugation with the amino groups on lysine residues of bitistatin, and the other for coordination of ^{99m}Tc. Bitistatin (0.22 mmol) was incubated for 90 min at room temperature with excess of *N*-succinimidyl-HYNIC (8.8 mmol). There were ~2 HYNIC molecules per bitistatin. After purification, 4.2 GBq/ml (113 mCi) of ^{99m}Tc-glucoheptonate was mixed with HYNIC-bitistatin. The mixture was incubated at for 30 min room temperature. Radiochemical purity was >97% after high-performance liquid chromatography with a specific activity of 96 TBq/mmol (2,600 Ci/mmol). Recombinant bitistatin (rBitistatin) has recently been radiolabeled with ^{99m}Tc-pertechnetate, using tricine as a coligand, with a radiochemical purity of >90% and a specific activity of up to 333 TBq/mmol (9,000 Ci/mmol) (6).

In Vitro Studies: Testing in Cells and Tissues

[PubMed]

In a saturation binding experiment, ^{99m}Tc-HYNIC-bitistatin exhibited a binding constant (K_d) of 32 ± 1 nM in human stimulated platelets, whereas resting platelets exhibited a K_d value of 62 ± 9 nM (5). On the other hand, there was no difference in the number of binding sites per platelet (B_{max}) between stimulated and resting platelets. ^{99m}Tc-HYNIC-bitistatin had similar binding affinity to that of ^{125}I-bitistatin (41 ± 5 and 56 ± 5 nM for stimulated and resting platelets, respectively).

Animal Studies

Rodents

[PubMed]

Knight et al. (6) performed biodistribution studies of ^{99m}Tc-HYNIC-rBitistatin in normal mice. The highest radioactivity concentrations were observed in the kidneys (90.9% injected dose per gram (ID/g)), spleen (10.6% ID/g), lungs (8.0% ID/g), blood (7.2% ID/g), and liver (4.8% ID/g) at 15 min after injection. With the exception of the intestines, all other organs and tissues showed a continuing decrease in radioactivity with time up to 4 h.

Other Non-Primate Mammals

[PubMed]

Knight et al. (6) performed biodistribution studies of ^{99m}Tc-HYNIC-rBitistatin in normal dogs. The highest radioactivity concentrations were observed in the kidneys (40.3% ID/organ), blood (23.42% ID/organ), liver (12.5% ID/organ) lungs (6.49% ID/organ), and spleen (3.75% ID/organ) at 4 h after injection; 87% of blood radioactivity was bound to platelets. Urine excretion averaged 23% of ID by 4 h after injection.

Knight et al. (5) performed SPECT planar imaging in dogs (n = 6) with DVT and PE induced by placing thrombogenic embolization coils in the right femoral vein. *In vivo*, focal uptake was observed as early as 30 min (DVT) and 60 min (PE) after injection. Lesion uptake of ^{99m}Tc-HYNIC-bitistatin at 4 h after injection averaged 0.89 ± 0.34% ID/g PE and 0.79 ± 0.23% ID/g DVT. Lesion/background ratios averaged 27 ± 13 (PE/blood), 34 ± 12 (PE/lung), 18 ± 4 (DVT/blood), and 284 ± 97 (DVT/muscle). The blood clearance pattern exhibited a two-phase model with a half-life ($t_{1/2}$α) of 8.9 min during the distribution phase and a half-life ($t_{1/2}$ß) of 5.8 h during the elimination phase.

Non-Human Primates

[PubMed]

No publication is currently available.

Human Studies

[PubMed]

Knight et al. (6) performed ^{99m}Tc-HYNIC-rBitistatin scintigraphy in 4 normal volunteers. The blood clearance pattern exhibited a two-phase model with a distribution half-life $t_{1/2}$α of 6.6 min and an elimination half-life $t_{1/2}$ß of 3.8 h. The organ with the highest accumulation was the kidney (5.3% ID), followed by the liver (4.1% ID) and spleen (2.7% ID) at 1 h. Urine excretion averaged 30% of ID by 4 h after injection. The effective dose equivalent was estimated to be 5.4 µSv/MBq (19.9 mrem/mCi) for adult males and 7.1 µSv/MBq (26.2 mrem/mCi) for adult females.

NIH Support

R01 HL54578, R01 HL054578-07, CA16520, DK19525

References

1. Corti R., Fuster V. *New understanding, diagnosis, and prognosis of atherothrombosis and the role of imaging.* . Am J Cardiol. 2003;91(3A):17A–26A. PubMed PMID: 12505565.
2. Taillefer R. *Radiolabeled peptides in the detection of deep venous thrombosis.* . Semin Nucl Med. 2001;31(2):102–23. PubMed PMID: 11330782.
3. Knight L.C., Romano J.E. *Functional expression of bitistatin, a disintegrin with potential use in molecular imaging of thromboembolic disease.* . Protein Expr Purif. 2005;39(2):307–19. PubMed PMID: 15642483.
4. Shebuski R.J., Ramjit D.R., Bencen G.H., Polokoff M.A. *Characterization and platelet inhibitory activity of bitistatin, a potent arginine-glycine-aspartic acid-containing peptide from the venom of the viper Bitis arietans.* . J Biol Chem. 1989;264(36):21550–6. PubMed PMID: 2600082.
5. Knight L.C., Baidoo K.E., Romano J.E., Gabriel J.L., Maurer A.H. *Imaging pulmonary emboli and deep venous thrombi with 99mTc-bitistatin, a platelet-binding polypeptide from viper venom.* . J Nucl Med. 2000;41(6):1056–64. PubMed PMID: 10855635.
6. Knight L.C., Romano J.E., Cosenza S.C., Iqbal N.M., Marcinkiewicz C. *Differences in binding of (99m)Tc-disintegrins to integrin alphavbeta3 on tumor and vascular cells.* . Nucl Med Biol. 2007;34(4):371–81. PubMed PMID: 17499726.